13

Minimal Market Model

This chapter derives an alternative model for the long term dynamics of the GOP from basic economic arguments. The discounted GOP drift, which models the long term trend of the economy, is chosen as the key parameter process. This leads to the minimal market model with the discounted GOP forming a time transformed squared Bessel process of dimension four. Its dynamics allows us to explain various empirical stylized facts and other properties relating to the long term behavior of a world stock index.

13.1 Parametrization via Volatility or Drift

Volatility Parametrization

The market portfolio can be interpreted as an accumulation index, or total return index. Let us again assume that a diversified stock market index approximates the GOP. The SDE (10.2.8) of the GOP reveals a close link between its drift and diffusion coefficient. More precisely, the risk premium of the GOP equals the square of its volatility. To see this clearly, we rewrite the SDE (10.2.8) for the discounted GOP when assuming a CFM, see Definition 10.1.2, in the form

$$d\bar{S}_t^{\delta_*} = \bar{S}_t^{\delta_*} |\theta_t| \left(|\theta_t| \, dt + dW_t\right), \tag{13.1.1}$$

where

$$dW_t = \frac{1}{|\theta_t|} \sum_{k=1}^{d} \theta_t^k \, dW_t^k \tag{13.1.2}$$

is the stochastic differential of a standard Wiener process W. For the efficient modeling of the GOP it is important to find an appropriate parametrization. The SDE (13.1.1) uses the *volatility parametrization* of the GOP, which can be best identified after application of a logarithmic transformation to $\bar{S}_t^{\delta_*}$. By taking the logarithm of the discounted GOP $\bar{S}_t^{\delta_*}$ we obtain from (13.1.1) the SDE

E. Platen, D. Heath, *A Benchmark Approach to Quantitative Finance*,
Springer Finance,

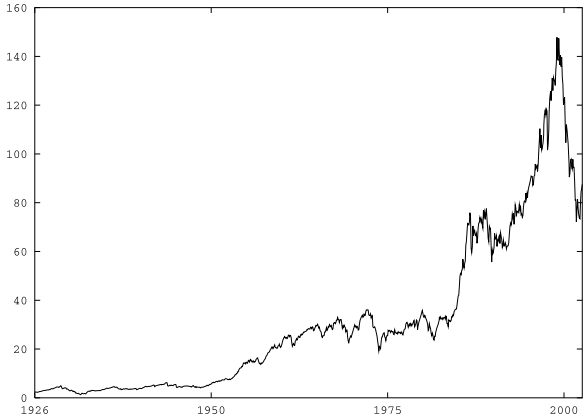

Fig. 13.1.1. Discounted WSI

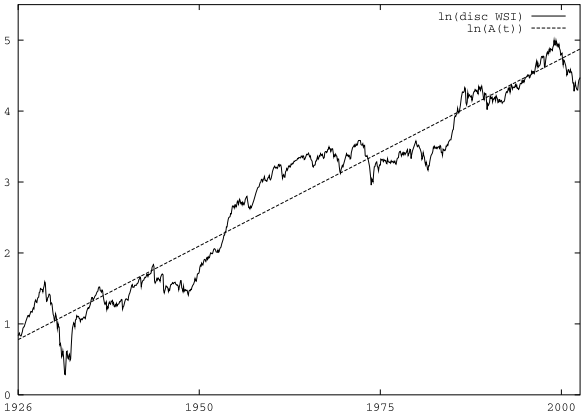

Fig. 13.1.2. Logarithm of discounted WSI

$$d\ln\left(\bar{S}_t^{\delta_*}\right) = \frac{1}{2}\,|\theta_t|^2\,dt + |\theta_t|\,dW_t \tag{13.1.3}$$

for $t \in [0,\infty)$, see Exercise 13.1. On the right hand side of this equation only one parameter process appears in the drift and diffusion coefficients.

Figure 13.1.1 shows a discounted world stock index (WSI) observed in US dollars from 1926 until 2004. This index starts at $\bar{S}_0^{\delta_*} = 2.3$ in January 1926 and has been reconstructed from monthly data provided by Global Financial Data.

The logarithm of the above discounted WSI is displayed in Fig. 13.1.2. One notes that the logarithm of the discounted WSI increases on average linearly with some fluctuations and could be potentially related to some underlying stationary process. One possibility is to model the logarithm of the discounted WSI by a simple time transformed Wiener process, a Lévy process or another process with independent increments. However, the increasing variance of such a process over time would not match the dynamics that we observe. Therefore,

there has to be some feedback effect modeled that drives the logarithm of the index back to its long-term average linear growth, consistent with stationary variance.

It is apparent that constant volatility is not compatible with stationary variance for the logarithm of the discounted WSI. Also if volatility is stochastic, stationary and independent of the driving noise of the WSI, then the variance of the logarithm of the WSI is going to increase over time. Thus, it would seem that some dependence between the WSI and its volatility needs to be established in a reasonable model for its long term dynamics.

Unfortunately, volatility does not have a major economic interpretation and is difficult to observe, see Corsi et al. (2001) and Barndorff-Nielsen & Shephard (2003). It simply emerges as a traditional parameter process in an attempt to model the random fluctuations or local risk of asset prices via the logarithmic transformation. The use of volatility as a parameter process grew historically from an early practice that employed geometric Brownian motion in the modeling of asset prices, see Osborne (1959), Samuelson (1971) and Black & Scholes (1973). However, in recent years growing concerns have emerged about the deficiencies of geometric Brownian motion as an asset price model. A major problem is the fact that volatility is, in reality, stochastic, see Fig. 12.1.1. Many other parameterizations of asset price dynamics are possible. Ideally, there should be an economically based or plausible parametrization which may then explain a potential link between the changes in the WSI and its volatility. As explained in Sect. 12.1, the volatility of an index has, via the leverage effect, some qualitative link to the value of the underlying index. Still, the leverage effect should also be explained on the basis of formal economic reasoning and, ideally, should be specified quantitatively.

Drift Parametrization

From an economic perspective it is clear that the WSI needs always to revert back to its underlying economic value even if this may take a long time. This property is a consequence of the conservation of value in an economy. We have observed that the drift of the discounted GOP can be interpreted as the change per unit of time of its underlying economic value. This drift provides an important link between the long term average evolution of the market index and the long term growth of the macro economy. By the law of conservation of value, the growth rate of the discounted index should in the long term, on average, match the growth rate of the total net wealth of the companies which comprise the market portfolio. Therefore, let us parameterize the discounted GOP dynamics, that is the SDE (13.1.1), by its trend. More precisely, we consider the *discounted GOP drift*

$$\alpha_t^{\delta_*} = \bar{S}_t^{\delta_*} |\theta_t|^2 \tag{13.1.4}$$

for $t \in [0, \infty)$, which is assumed to be a strictly positive, predictable parameter process, see (11.1.4). Using this parametrization we obtain from (13.1.4) the

volatility $|\theta_t|$ of the GOP in the form

$$|\theta_t| = \sqrt{\frac{\alpha_t^{\delta_*}}{\bar{S}_t^{\delta_*}}}. \tag{13.1.5}$$

This structure provides a natural explanation for the leverage effect. When the index decreases, then the volatility increases and vice versa. This creates a feedback effect resulting from the structure of the SDE (13.1.1) for the discounted GOP.

By substituting (13.1.4) and (13.1.5) into (13.1.1), we obtain the following parametrization of the SDE of the discounted GOP:

$$d\bar{S}_t^{\delta_*} = \alpha_t^{\delta_*}\, dt + \sqrt{\bar{S}_t^{\delta_*}\, \alpha_t^{\delta_*}}\, dW_t \tag{13.1.6}$$

for $t \in [0, \infty)$. We emphasize that the square root of the discounted GOP appears in the diffusion coefficient. Note that the parameter process $\alpha^{\delta_*} = \{\alpha_t^{\delta_*}, t \in [0, \infty)\}$ can be freely specified as a predictable stochastic process such that the SDE (13.1.6) has a unique strong solution.

With the quantity

$$A_t = A_0 + \int_0^t \alpha_s^{\delta_*}\, ds \tag{13.1.7}$$

we can rewrite (13.1.6) in the form

$$\bar{S}_t^{\delta_*} = \bar{S}_0^{\delta_*} + A_t - A_0 + \int_0^t \sqrt{\bar{S}_s^{\delta_*}\, \alpha_s^{\delta_*}}\, dW_s \tag{13.1.8}$$

for $t \in [0, \infty)$. Here A_t can be interpreted as the *underlying value* at time t of the discounted GOP, where A_0 needs to be appropriately chosen as the initial underlying value at time $t = 0$. One can say that the underlying value A_t corresponds to the discounted wealth that underlies the discounted index $\bar{S}^{\delta_*}$. The drift parametrization above has, therefore, a formal economic meaning. If one expects the fluctuations of the increase per unit of time of the discounted underlying value to be reasonably independent of trading uncertainty, then the fitting of a model to market data is more likely to be effective and amenable to this drift parametrization rather than to the alternative formulation using volatility.

Squared Bessel Process of Dimension Four

It is important to realize that the SDE (13.1.6) describes a very particular time transformed diffusion process. More precisely, it is the SDE of a time transformed squared Bessel process of dimension four, see Sect. 8.7 and Revuz & Yor (1999).

More precisely, with the specification of transformed time $\varphi(t)$ as

$$\varphi(t) = \frac{1}{4} \int_0^t \alpha_s^{\delta_*} \, ds \tag{13.1.9}$$

and with

$$X_{\varphi(t)} = \bar{S}_t^{\delta_*} \tag{13.1.10}$$

we obtain from (13.1.6) the SDE of a squared Bessel process of dimension four in the form

$$dX_{\varphi(t)} = 4\, d\varphi(t) + 2\sqrt{X_{\varphi(t)}}\, dW(\varphi(t)), \tag{13.1.11}$$

see (8.7.1), where

$$dW(\varphi(t)) = \sqrt{\frac{\alpha_t^{\delta_*}}{4}}\, dW_t \tag{13.1.12}$$

for $t \in [0, \infty)$. By (13.1.9) the increase of the transformed time equals a quarter of the underlying value A_t. This provides a simple economically founded parametrization of the discounted GOP dynamics. In the model the transformed time can be interpreted as business time or market time.

Note that we have still not specified the dynamics of the discounted GOP $\bar{S}_t^{\delta_*}$ because we have not fixed the dynamics of the discounted GOP drift process $\alpha_t^{\delta_*}$. So far almost any strictly positive, predictable process is possible here. The discounted GOP dynamics are in (13.1.6) and (13.1.11) only parameterized in an alternative way by using the drift instead of the volatility as parameter process.

Time Transformed Bessel Process

By application of the Itô formula to the square root of the discounted GOP one obtains from (13.1.6) the SDE

$$d\sqrt{\bar{S}_t^{\delta_*}} = \frac{3\,\alpha_t^{\delta_*}}{8\sqrt{\bar{S}_t^{\delta_*}}}\, dt + \frac{1}{2}\sqrt{\alpha_t^{\delta_*}}\, dW_t, \tag{13.1.13}$$

see Exercise 13.2. This is the SDE of a time transformed Bessel process of dimension four, see (7.7.19). In a CFM the quadratic variation of $\sqrt{\bar{S}^{\delta_*}}$ equals

$$\left[\sqrt{\bar{S}^{\delta_*}}\right]_t = \frac{1}{4} \int_0^t \alpha_s^{\delta_*} \, ds \tag{13.1.14}$$

for $t \in [0, \infty)$, see Sect. 5.2. This means that by (13.1.9) in a CFM the increment of the transformed time $\varphi(t)$ equals the quadratic variation of the time transformed Bessel process $\sqrt{\bar{S}^{\delta_*}}$. That is

$$\varphi(t) - \varphi(0) = \left[\sqrt{\bar{S}^{\delta_*}}\right]_t \tag{13.1.15}$$

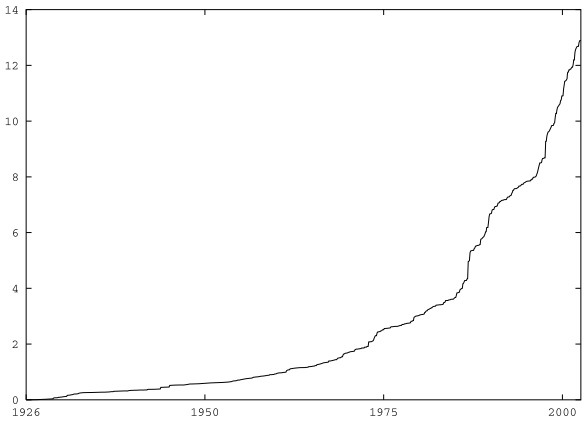

Fig. 13.1.3. Empirical quadratic variation of the square root of the discounted WSI

for $t \in [0, \infty)$. This is a surprisingly simple relationship. Hence, the transformed time process can be determined, in principle, from the quadratic variation of the square root of the discounted GOP, an observable quantity if we take the WSI as proxy for the GOP. For the discounted WSI shown in Fig. 13.1.1 we plot in Fig. 13.1.3 the empirical quadratic variation of its square root. One notes a reasonably smooth increase of this quadratic variation over the long time period.

We emphasize that so far we have not made any assumptions about the particular dynamics of the discounted GOP. The relationships revealed under the given drift parametrization hold generally for any CFM. In the next section we shall choose the discounted GOP drift as having a simple exponential function of time.

13.2 Stylized Minimal Market Model

Let us now apply the above results for the derivation of a parsimonious index model, the *minimal market model* (MMM), see Platen (2001, 2002, 2006c) and Sect. 7.5.

Net Growth Rate

By conservation of value the long-term growth rate of the underlying value of the discounted GOP can be expected to correspond to the long-term net growth rate of the world economy. According to historical records we assume in the long term, as a first approximation, that the world economy has been growing exponentially, see Fig. 13.1.2. Such exponential growth will now be postulated for the discounted GOP drift. The following assumption leads us to the stylized version of the MMM.

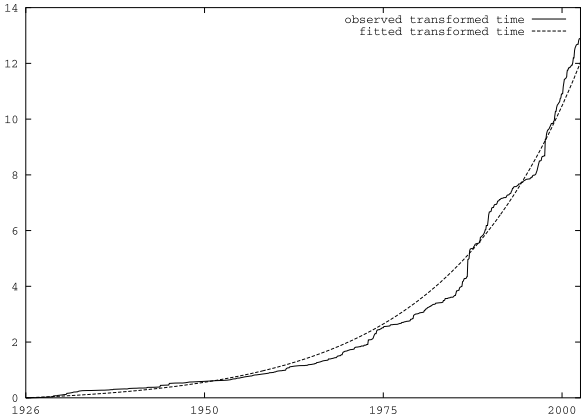

Fig. 13.2.1. Fitted and observed transformed time

Assumption 13.2.1. *The discounted GOP drift is an exponentially growing function of time.*

Note that this assumption can be considerably weakened and made more flexible, as will be shown later in Sect. 13.4, see also Heath & Platen (2005b). To satisfy Assumption 13.2.1 let us model the discounted GOP drift $\alpha_t^{\delta_*}$ as an exponential function of time of the form

$$\alpha_t^{\delta_*} = \alpha_0 \exp\{\eta\, t\} \tag{13.2.1}$$

for $t \in [0, \infty)$. In this equation we have as parameters, a nonnegative *initial value* $\alpha_0 > 0$ and a constant *net growth rate* $\eta > 0$. Note that the initial value parameter α_0 depends on the initial date and also on the initial value of the discounted GOP. By equations (13.1.9) and (13.2.1) the underlying value at time t satisfies under the given parametrization the equation

$$\varphi(t) = \frac{\alpha_0}{4} \int_0^t \exp\{\eta\, z\}\, dz \tag{13.2.2}$$

for $t \in [0, \infty)$. This demonstrates that the transformed time and the underlying value evolve asymptotically for long time periods in an exponential manner. More precisely, one obtains for the transformed time the explicit expression

$$\varphi(t) = \frac{\alpha_0}{4\,\eta} \left(\exp\{\eta\, t\} - 1\right). \tag{13.2.3}$$

By applying standard curve fitting methods, see Sect. 2.3, we fit the transformed time $\varphi(t)$, satisfying (13.2.3), to the observed quadratic variation of the square root of the discounted WSI shown in Fig. 13.1.3. In Fig. 13.2.1 we plot then the resulting fit for the parameter choice $\alpha_0 = 0.043$ and $\eta = 0.0528$. One notes that we achieve a reasonable fit of the theoretical transformed time when only using a constant net growth rate η over the long time period.

The net growth rate for the market capitalization weighted world stock portfolio, when discounted by the US dollar savings account, has been estimated for the entire last century in Dimson et al. (2002) to be on average close to 0.049 under discrete annual compounding. This is reasonably close to what we have obtained as the annual net growth rate parameter $\eta = 0.0528$ under continuous compounding, as shown in Fig. 13.2.1.

Normalized GOP

We now discuss the feedback effect in the dynamics of the market index that drives its value back to its long term exponentially growing average. The formulation (13.2.1) suggests that one should examine for this purpose the *normalized GOP*

$$Y_t = \frac{\bar{S}_t^{\delta_*}}{\alpha_t^{\delta_*}} \tag{13.2.4}$$

for $t \in [0, \infty)$.

By application of the Itô formula and using (13.1.5) and (13.1.6), we obtain for this case the SDE

$$dY_t = (1 - \eta\, Y_t)\, dt + \sqrt{Y_t}\, dW_t \tag{13.2.5}$$

for $t \in [0, \infty)$ with

$$Y_0 = \frac{\bar{S}_0^{\delta_*}}{\alpha_0}, \tag{13.2.6}$$

see Exercise 13.3. Note by (8.7.34) that Y is a square root (SR) process of dimension four. The above stylized version of the MMM is an economically based, parsimonious model for the dynamics of the discounted GOP, and by extension for a WSI. We remark that we would still obtain the above type of SDE for Y_t if η were a stochastic process. This is rather important for extended versions of the MMM.

By using the SR process $Y = \{Y_t,\, t \in [0, \infty)\}$ and (13.2.5), the discounted GOP $\bar{S}_t^{\delta_*}$ can be expressed in the form

$$\bar{S}_t^{\delta_*} = Y_t\, \alpha_t^{\delta_*} \tag{13.2.7}$$

for $t \in [0, \infty)$. This leads us to a useful description of the GOP when expressed in units of the domestic currency given by

$$S_t^{\delta_*} = S_t^0\, \bar{S}_t^{\delta_*} = S_t^0\, Y_t\, \alpha_t^{\delta_*} \tag{13.2.8}$$

for $t \in [0, \infty)$. For the above model of the discounted GOP one needs only to specify the initial values $\bar{S}_0^{\delta_*}$ and α_0 and the net growth rate process η. Note that α_0 and $\bar{S}_0^{\delta_*}$ are linked through (13.2.6). Consequently, one can say that the stylized MMM assumes that the discounted GOP is the product of an SR process and an exponential function.

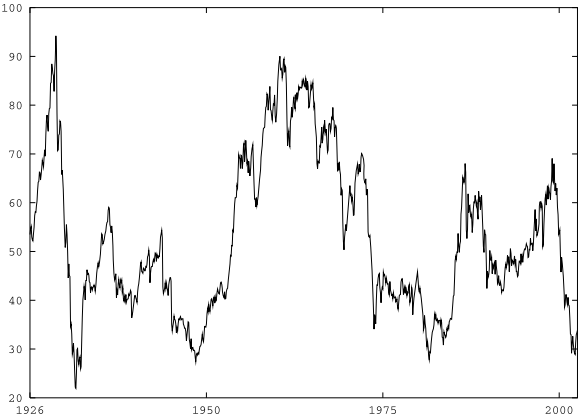

Fig. 13.2.2. Normalized GOP

One notes that the normalized GOP is an SR process of dimension four, see Sects. 4.4 and 7.5. The net growth rate η is here the speed of adjustment parameter for the linear mean-reversion. Note that besides the scalar initial values α_0 and $\bar{S}_0^{\delta_*}$, the net growth rate η is the only parameter process needed for the characterization of the dynamics of the normalized GOP under the MMM.

According to our previous findings for the discounted WSI shown in Fig. 13.1.1 we set $\eta = 0.0528$ and choose $\alpha_0 = 0.043$. With this parameter choice we show in Fig. 13.2.2 the resulting normalized GOP Y_t, constructed according to (13.2.4) and (13.2.1).

For the above choice of η the half life time of a major displacement of the normalized GOP would be about $\frac{\ln(2)}{\eta} \approx 13$ years. This rather long time period supports the view that it takes on average significant time to correct for major up- or downturns in the world financial market. One realizes that a look at the market performance over the last 10 or even 15 years may not be sufficient to judge its potential long term evolution. This is consistent with the impression that one obtains when studying in Fig. 13.1.2 the logarithm of the world stock index for the long period from 1926 until 2003. It seems to take about 25 years in this graph to go through a full "cycle" of random ups and downs for the market index. The MMM reflects well this type of long term mean reverting dynamics of the normalized GOP.

Since the normalized GOP Y_t has for constant net growth rate a stationary density, so has $\ln(Y_t)$. This means, that $\ln(Y_t)$ has a uniformly bounded variance for all $t \in [0, \infty)$. In this sense the stylized MMM with constant parameters exhibits some kind of an equilibrium dynamic. By taking the logarithm on both sides of equation (13.2.7) we obtain the relation

$$\ln(\bar{S}_t^{\delta_*}) = \ln(Y_t) + \ln(\alpha_0) + \eta\, t \tag{13.2.9}$$

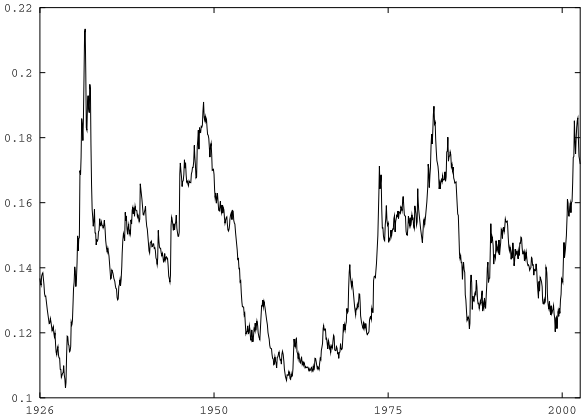

Fig. 13.2.3. Volatility of the WSI under the MMM

for $t \in [0, \infty)$, assuming the net growth rate to be a constant. The above stylized MMM suggests the logarithm of the discounted GOP will fluctuate around a straight line with slope η. The variance of $\ln(\bar{S}_t^{\delta_*})$ is therefore uniformly bounded under the MMM. This is also what one observes in Fig. 13.1.2.

The BS model and most of its extensions, with volatility processes independent of the trading noise, are not able to recover dynamics of the type shown in Fig. 13.1.2. In particular, exponential Lévy models, as mentioned in Sect. 3.6, share this problem. Stochastic volatility models, as discussed in Sect. 12.4, are better suited. However, they need an extra volatility process to generate some negative correlation between volatility and index as described earlier. The MMM is a parsimonious model that does not need any extra volatility process, but still generates a realistic long term dynamics for the GOP.

Volatility under the MMM

The resulting model for the discounted GOP with constant net growth rate η is called the stylized version of the MMM, which was originally proposed in Platen (2001). We now discuss the endogenous nature of volatility as it emerges under the MMM.

According to formula (13.2.4), under the MMM the discounted GOP has the volatility

$$|\theta_t| = \frac{1}{\sqrt{Y_t}} \tag{13.2.10}$$

for $t \in [0, \infty)$. We plot in Fig. 13.2.3 the path of the volatility for the discounted WSI, shown in Fig. 13.1.1, as it follows under the MMM for the default parameters $\eta = 0.0528$ and $\alpha_0 = 0.043$. It is interesting to note that according to this graph the volatility was, for instance, relatively high around 1975 and rather low during the period near the year 2000. The stochastic

volatility process of the WSI under the MMM, as shown in Fig. 13.2.3, is negatively correlated to the normalized WSI and, therefore, also negatively correlated to the WSI.

From (13.2.10) and (13.2.5) it can be seen that the squared volatility $|\theta_t|^2$ satisfies the SDE

$$d|\theta_t|^2 = d\left(\frac{1}{Y_t}\right) = |\theta_t|^2 \eta \, dt - \left(|\theta_t|^2\right)^{\frac{3}{2}} dW_t \tag{13.2.11}$$

for $t \in [0, \infty)$, see Exercise 13.4. This provides us with a stochastic volatility model in the sense as discussed in Sect. 12.4. Note that the diffusion coefficient of the squared volatility has in (13.2.11) the power $\frac{3}{2}$. In Platen (1997) such a 3/2 volatility model was suggested for the modeling of a market index, see also (12.4.24). This stochastic volatility model has been obtained under the benchmark approach by using economic arguments.

Distribution of Log-Returns under the MMM

Let us now examine the distribution of log-returns of the GOP that can be expected to be estimated under the MMM. We show that under the MMM the estimated log-returns of the GOP, from sufficiently long observation periods, are Student t distributed with four degrees of freedom. To see this, let us recall that under the MMM the squared volatility of the GOP is by (13.2.4) given as

$$|\theta_t|^2 = \frac{1}{Y_t}, \tag{13.2.12}$$

which is the inverse of an SR process. Note from (4.5.7) that the SR process Y has as stationary density a gamma density with four degrees of freedom. Consequently, the squared volatility $\frac{1}{Y_t}$ has an *inverse gamma density* as its stationary density.

When estimating the density of, say, daily log-returns that are observed over a long time period, then the stationary density of the squared volatility acts as mixing density for the stochastic variance of the log-returns. This is similar to normal variance mixture models, as discussed in Sect. 2.5, and to stochastic volatility models, as described in Sect. 12.4. We refer also to Kessler (1997), Prakasa Rao (1999) and Kelly, Platen & Sørensen (2004) for more details on this issue. For log-returns of the GOP, the inverse gamma density acts under the MMM as a mixing density for their normal-mixture distribution. It follows from (1.2.16) and (1.2.28) that the resulting normal-mixture distribution is the Student t distribution with four degrees of freedom. Therefore, this is the theoretically predicted log-return density that will be estimated under the stylized MMM dynamics. We emphasize that one needs a sufficiently long time period with log-return observations for this kind of estimation procedure to be reliable. Obviously, the path of the ergodic process $\frac{1}{Y}$ needs enough time to sufficiently act in its mixing role for the random

variance of the conditionally Gaussian log-returns. Since we have seen that the half life time of shocks on the square root process Y for the calibrated MMM is about 13 years, the available 33 years of daily data can be possibly considered to be just sufficient to confirm or reject the predicted Student t feature of log-returns.

The above described distributional feature of the MMM is rather clear and testable. Most importantly, the Student t log-return property has already been documented in the literature as an empirical stylized fact, as was pointed out in Sect. 2.6. Recall that Markowitz & Usmen (1996a) found that the Student t distribution with about 4.5 degrees of freedom matches daily S&P500 log-return data well. Hurst & Platen (1997) found within the rich class of symmetric generalized hyperbolic distributions that for most stock market indices, daily log-returns are likely to be Student t distributed with about four degrees of freedom. Fergusson & Platen (2006) confirmed with high accuracy this empirical stylized fact. Furthermore, in Breymann et al. (2003) the copula, see Sect. 1.5, of the joint distribution of log-returns of exchange rates has been identified as a Student t copula with roughly four degrees of freedom. One can say that the MMM provides in its stylized version a rather accurate model for the probabilistic nature of the log-returns of a world stock index.

Stylized Multi-Currency MMM (*)

We have examined under the MMM the properties of stochastic volatility for the discounted GOP in a currency denomination. By using the same arguments as above, we now show how to model exchange rates. This will result in a stylized multi-currency version of the MMM, similar to the one described in Platen (2001) and Heath & Platen (2005a).

Let us consider a market with $d+1$ currencies, $d \in \mathcal{N}$. We denote by $S_i^{\delta_*}(t)$ the GOP at time t when denominated in units of the ith currency, $i \in \{0, 1, \ldots, d\}$. Furthermore, r_t^i is the short rate for the ith currency and $\theta_i^k(t)$ the market price of risk for the ith currency denomination with respect to the kth Wiener process, $k \in \{1, 2, \ldots, d+1\}$, $t \in [0, \infty)$.

We derive now a stylized multi-currency version of the MMM. Assuming, for simplicity, constant net growth rates and constant short rates, we can describe at time t the value of the GOP in the ith currency denomination according to (13.2.8) by the expression

$$S_i^{\delta_*}(t) = \alpha_t^i \, Y_t^i \, S_i^i(t). \tag{13.2.13}$$

Here we have

$$\alpha_t^i = \alpha_0^i \, \exp\{\eta^i \, t\}, \tag{13.2.14}$$

$$S_i^i(t) = \exp\{r^i \, t\}. \tag{13.2.15}$$

The ith normalized GOP Y_t^i satisfies the SDE

$$dY_t^i = \left(1 - \eta^i\, Y_t^i\right) dt + \sqrt{Y_t^i} \sum_{k=1}^{d+1} q^{i,k}\, dW_t^k \tag{13.2.16}$$

for $t \in [0, \infty)$, with $Y_0^i > 0$ and η^i the ith net growth rate, $i \in \{0, 1, \ldots, d\}$. Furthermore, we introduce constant *scaling levels* $q^{i,k}$, for $i \in \{0, 1, \ldots, d\}$ and $k \in \{1, 2, \ldots, d+1\}$ to model the covariations between normalized GOPs Y^i and Y^j for $i \neq j$. For the stylized multi-currency version of the MMM we set, for simplicity,

$$\sum_{k=1}^{d+1} (q^{i,k})^2 = 1 \tag{13.2.17}$$

for all $i \in \{0, 1, \ldots, d\}$. This constraint can be relaxed in extended versions of the MMM.

The (i, j)th exchange rate $X_t^{i,j}$ from the jth into the ith currency is given at time t by the ratio

$$X_t^{i,j} = \frac{S_i^{\delta_*}(t)}{S_j^{\delta_*}(t)} = \frac{Y_t^i\, \alpha_t^i\, S_i^i(t)}{Y_t^j\, \alpha_t^j\, S_j^j(t)}. \tag{13.2.18}$$

This satisfies the SDE

$$dX_t^{i,j} = X_t^{i,j} \left((r^i - r^j)\, dt + \sum_{k=1}^{d+1} \left(\frac{q^{i,k}}{\sqrt{Y_t^i}} - \frac{q^{j,k}}{\sqrt{Y_t^j}} \right) \left(\frac{q^{i,k}}{\sqrt{Y_t^i}}\, dt + dW_t^k \right) \right) \tag{13.2.19}$$

for $t \in [0, \infty)$ with $X_0^{i,j} > 0$, $i, j \in \{0, 1, \ldots, d\}$. Hence, this is the dynamics for an exchange rate, consistent with that of the GOP having the structure (13.2.13) and (13.2.16) in each currency denomination. Under the multi-currency MMM the exchange rate volatility depends on the volatilities of the GOPs in both currencies and, thus, on the fluctuations of the GOP in both denominations.

The jth savings account, when denominated in the ith currency, is given by the product

$$S_i^j(t) = X_t^{i,j}\, S_j^j(t). \tag{13.2.20}$$

Consequently, by the Itô formula it satisfies the SDE

$$dS_i^j(t) = S_i^j(t) \left(r^i\, dt + \sum_{k=1}^{d+1} \left(\frac{q^{i,k}}{\sqrt{Y_t^i}} - \frac{q^{j,k}}{\sqrt{Y_t^j}} \right) \left(\frac{q^{i,k}}{\sqrt{Y_t^i}}\, dt + dW_t^k \right) \right) \tag{13.2.21}$$

for all $t \in [0, \infty)$ with $S_i^j(0) > 0$ for $i, j \in \{0, 1, \ldots, d\}$.

One notes from (10.1.7) that the stochastic market price of risk with respect to the kth Wiener process under the ith currency denomination is of the form

$$\theta_i^k(t) = \frac{q^{i,k}}{\sqrt{Y_t^i}} \tag{13.2.22}$$

for all $t \in [0, \infty)$, $i \in \{0, 1, \ldots, d\}$ and $k \in \{1, 2, \ldots, d+1\}$. The (j,k)th volatility in the ith denomination is given by the expression

$$b_i^{j,k}(t) = \theta_i^k(t) - \theta_j^k(t) \tag{13.2.23}$$

for $t \in [0, \infty)$, $i, j \in \{0, 1, \ldots, d\}$ and $k \in \{1, 2, \ldots, d+1\}$ and is, therefore, stochastic. One notes that the volatility of an exchange rate is different and more complex than that of an index. The interplay between the volatilities of the denominations of the GOP in two different currencies under the MMM is visible in the above volatility structure of the corresponding exchange rate.

In fact, the above stylized multi-currency MMM, which characterizes a currency market, can be used to model an equity market. For equity markets the exdividend spot price of a stock is treated in the same manner as an exchange rate. The share savings account of a cum dividend stock is then similar to that of a foreign savings account. The dividend rate plays a similar role to that of the short rate for a foreign savings account. In Platen & Stahl (2003) it is shown that log-returns of many benchmarked US stocks are Student t distributed with about four degrees of freedom. This suggests that, potentially, the above stylized multi-currency MMM can also be applied to a number of stocks.

In this context it is worth mentioning that the spot price of a commodity, like gold, copper, oil or electricity, can also be modeled like an exchange rate. Here, the, so-called, convenience yield, see Miltersen & Schwartz (1998), behaves in a similar manner as the foreign short rate. In this sense the above stylized multi-currency MMM can be used to model commodity prices. Forthcoming work will identify the dynamics of the GOP when denominated in units of equities or commodities.

13.3 Derivatives under the MMM

This section derives pricing formulas for standard derivatives under the stylized MMM. This includes zero coupon bonds, as well as, call and put options on an index. In this section we rely on the methodology presented in Chap. 12.

Zero Coupon Bond under the MMM

First, we study the price of a zero coupon bond under the stylized MMM. For simplicity, we assume that the short rate r_t is deterministic and the net growth rate η is constant. The price $P(t,T)$ of a zero coupon bond that matures at time $T \in (0, \infty)$ is by the real world pricing formula (9.1.34) and (10.4.1) obtained from the conditional expectation

$$P(t,T) = S_t^{\delta_*} \, E\left(\frac{1}{S_T^{\delta_*}} \,\middle|\, \mathcal{A}_t \right) = \exp\left\{ - \int_t^T r_s \, ds \right\} E\left(\frac{\bar{S}_t^{\delta_*}}{\bar{S}_T^{\delta_*}} \,\middle|\, \mathcal{A}_t \right) \tag{13.3.1}$$

for $t \in [0,T]$. We recall that the discounted GOP $\bar{S}^{\delta_*}$ is a time transformed squared Bessel process of dimension $\delta = 4$. As in (13.2.1) we choose the discounted GOP drift

$$\alpha_t^{\delta_*} = \alpha_0 \, \exp\{\eta \, t\} \tag{13.3.2}$$

with initial value $\alpha_0 > 0$ and constant net growth rate $\eta > 0$. The corresponding time transformation is given in (13.2.3) by

$$\varphi(t) = \frac{\alpha_0}{4\,\eta} \left(\exp\{\eta \, t\} - 1 \right) \tag{13.3.3}$$

for $t \in [0, \infty)$, where we set $\varphi(0) = 0$. We know by the formula (8.7.17) the first negative moment of a squared Bessel process of dimension $\delta = 4$, which has the form

$$E\left(\left(\bar{S}_T^{\delta_*} \right)^{-1} \,\middle|\, \mathcal{A}_t \right) = \left(\bar{S}_t^{\delta_*} \right)^{-1} \left(1 - \exp\left\{ - \frac{\bar{S}_t^{\delta_*}}{2\,(\varphi(T) - \varphi(t))} \right\} \right). \tag{13.3.4}$$

Therefore, we obtain by (13.3.1) and (13.3.4) the price for the fair zero coupon bond

$$P(t,T) = \exp\left\{ - \int_t^T r_s \, ds \right\} \left(1 - \exp\left\{ - \frac{\bar{S}_t^{\delta_*}}{2\,(\varphi(T) - \varphi(t))} \right\} \right) \tag{13.3.5}$$

for $t \in [0,T)$. Hence, for the stylized MMM an explicit formula exists for the price of a zero coupon bond, which was originally derived in Platen (2002).

Forward Rates under the MMM

As introduced in Sect. 10.4, the forward rate $f(t,T)$ at time t for the maturity date $T \in (0, \infty)$ is given by the formula

$$f(t,T) = - \frac{\partial}{\partial T} \ln(P(t,T)) \tag{13.3.6}$$

for $t \in [0,T)$. Using (13.3.5) for the stylized MMM with deterministic short rate, the forward rate follows in the form

$$f(t,T) = r_T + n(t,T), \tag{13.3.7}$$

where $n(t,T)$ describes the *market price of risk contribution*

$$n(t,T) = - \frac{\partial}{\partial T} \ln\left(1 - \exp\left\{ - \frac{\bar{S}_t^{\delta_*}}{2(\varphi(T) - \varphi(t))} \right\} \right). \tag{13.3.8}$$

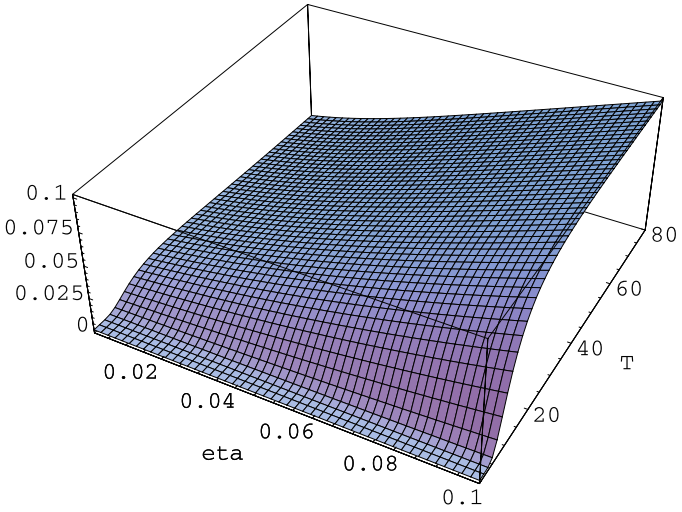

Fig. 13.3.1. Market price of risk contribution in dependence on η and T

In our case with a deterministic short rate, the forward rate is the sum of the short rate at the maturity date and the market price of risk contribution. The existence of a nonzero market price of risk contribution is a consequence of the fact that the stylized MMM does not have an equivalent risk neutral probability measure. By performing the differentiation in (13.3.8) we obtain the equation

$$\begin{aligned} n(t,T) &= \frac{1}{\left(\exp\left\{\frac{\bar{S}_t^{\delta_*}}{2(\varphi(T)-\varphi(t))}\right\}-1\right)} \frac{\bar{S}_t^{\delta_*}}{\left(\varphi(T)-\varphi(t)\right)^2} \frac{\alpha_T^{\delta_*}}{8} \\ &= \frac{2\,\eta^2\,Y_t}{\left(\exp\left\{\frac{2\,\eta\,Y_t}{(\exp\{\eta\,(T-t)\}-1)}\right\}-1\right)\left(\exp\{\eta\,(T-t)\}-1\right)} \\ &\quad \times \frac{1}{\left(1-\exp\{-\eta\,(T-t)\}\right)} \end{aligned} \tag{13.3.9}$$

for $t \in [0,T)$, $T \in (0,\infty)$.

To illustrate the type of market price of risk contribution that the stylized MMM produces we plot in Fig. 13.3.1 this function for $t = 0$ and $Y_0 = 53$ as a function of the net growth rate $\eta \in [0.001, 0.1]$ and the maturity $T \in [0.001, 80.0]$. It can be seen that the market price of risk contribution is practically zero for short dated maturities of up to one or two years. Afterwards, one obtains an increase in the value of the market price of risk contribution. For larger net growth rates the market price of risk contribution is larger. For extremely large time to maturity it equals the net growth rate, that is,

$$\lim_{T\to\infty} n(t,T) = \eta. \tag{13.3.10}$$

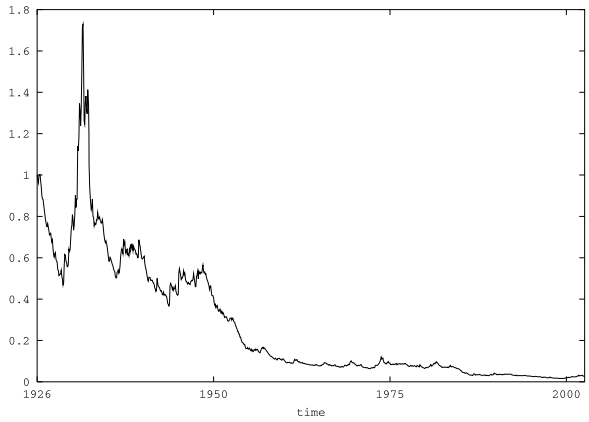

Fig. 13.3.2. Candidate Radon-Nikodym derivative for world market

In Platen (2005a) and Miller & Platen (2005) interest rate term structure models are discussed that are based on versions of the MMM.

Absence of an Equivalent Risk Neutral Probability Measure

From the fair bond price (13.3.5) we note for $t \in [0, T)$ that

$$P(t,T) < P_T^*(t) = \exp\left\{-\int_t^T r_s \, ds\right\} = \frac{S_t^0}{S_T^0}, \tag{13.3.11}$$

which means for the stylized MMM that the fair zero coupon bond has a lower price than the savings bond $P_T^*(t)$. As discussed in the previous chapter, this demonstrates that the stylized MMM does not have an equivalent risk neutral probability measure. Indeed, the candidate Radon-Nikodym derivative process $\Lambda = \{\Lambda_t, \, t \in [0, \infty)\}$ for the hypothetical risk neutral measure, where

$$\Lambda_t = \frac{\hat{S}_t^0}{\hat{S}_0^0} = \frac{\bar{S}_0^{\delta_*}}{\bar{S}_t^{\delta_*}}, \tag{13.3.12}$$

is a strict $(\underline{\mathcal{A}}, P)$-supermartingale. This follows from our example in Sect. 8.7 for the inverse of a squared Bessel process of dimension four. Consequently, by Lemma 5.2.3 the process Λ is a strict supermartingale. In Fig. 13.3.2 we show the candidate Radon-Nikodym derivative for the world market from 1926 until 2004, as it results when interpreting the discounted WSI in Fig. 13.1.1 as discounted GOP. We have for the hypothetical risk neutral measure P_θ on $[0, T]$ the inequality

$$P_{\theta,T}(\Omega) = E\left(\Lambda_T \,\middle|\, \mathcal{A}_0\right) = 1 - \exp\left\{-\frac{\bar{S}_0^{\delta_*}}{2\,\varphi(T)}\right\} < \Lambda_0 = 1. \tag{13.3.13}$$

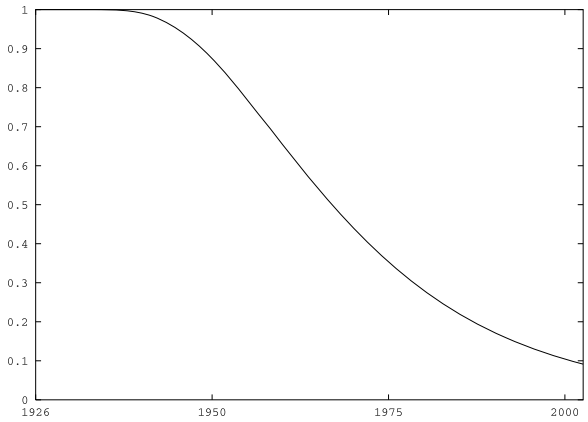

Fig. 13.3.3. Total mass of a hypothetical risk neutral measure

This shows that P_θ is not a probability measure because it does not give a total mass of one, see (1.1.4). This important fact does not create a problem, since we shall use the real world pricing formula to obtain derivative prices under the MMM and do not rely on risk neutral pricing. For illustration we show in Fig. 13.3.3 the total mass of the candidate risk neutral measure $P_\theta(\Omega)$ as a function of T. Here we use the default parameters $\eta = 0.0528$, $\alpha_0 = 0.043$ and $\bar{S}_0^{\delta_*} = 2.3$. One notes that the difference in total probability mass from the value one is very small for short time horizons T of up to about ten years. In this range the hypothetical risk neutral measure is almost a probability measure. However, after ten years we observe the begin of a significant decline. After 40 years the total mass of the hypothetical risk neutral measure is only about 0.5. In these circumstances it is then not reasonable to expect a "risk neutral" price to be realistic for time horizons beyond ten years.

Transition Density of the Stylized MMM

Before we price any particular European option we recall the transition density of the discounted GOP $\bar{S}^{\delta_*}$. According to (8.7.9) this transition density is of the form

$$p(s,x;t,y) = \frac{1}{2\,(\varphi(t)-\varphi(s))} \left(\frac{y}{x}\right)^{\frac{1}{2}} \exp\left\{-\frac{x+y}{2\,(\varphi(t)-\varphi(s))}\right\} I_1\left(\frac{\sqrt{x\,y}}{\varphi(t)-\varphi(s)}\right) \tag{13.3.14}$$

for $0 \le s < t < \infty$ and $x, y \in (0,\infty)$. Here $I_1(\cdot)$ is the modified Bessel function of the first kind with index $\nu = 1$, see (1.2.15). Note by (1.2.14) that (13.3.14) is the density of a non-central chi-square distributed random variable at time t with value

$$\frac{y}{\varphi(t)-\varphi(s)} = \frac{\bar{S}_t^{\delta_*}}{\varphi(t)-\varphi(s)}$$

with $\delta = 4$ degrees of freedom and non-centrality parameter

$$\frac{x}{\varphi(t)-\varphi(s)} = \frac{\bar{S}^{\delta_*}_s}{\varphi(t)-\varphi(s)}.$$

Recall that Fig. 8.7.2 shows the transition density of a squared Bessel process of dimension four.

It is also interesting to consider the transition density for the normalized GOP

$$Y_t = \frac{\bar{S}^{\delta_*}_t}{\alpha^{\delta_*}_t},$$

see (13.2.4). This density is by (8.7.44) of the form

$$p(s,x;t,y) = \frac{1}{2\,\bar{s}_t\,\bar{\varphi}_t}\left(\frac{y}{x\,\bar{s}_t}\right)^{\frac{1}{2}} \exp\left\{-\frac{x+\frac{y}{\bar{s}_t}}{2\,\bar{\varphi}_t}\right\} I_1\left(\frac{\sqrt{x\,\frac{y}{\bar{s}_t}}}{\bar{\varphi}_t}\right) \tag{13.3.15}$$

for $0 \le s < t < \infty$ and $x, y \in (0,\infty)$, where $\bar{s}_t = \exp\{-\eta(t-s)\}$ and $\bar{\varphi}_t = \frac{1}{4\eta}(\exp\{\eta(t-s)\}-1)$. Recall that Fig. 4.4.1 shows the transition density of a square root process of dimension $\delta = 4$.

European Call Options under the MMM

Since a diversified index is considered to be a proxy for the GOP, see Sect. 10.6, the MMM would appear to be a reasonable choice to model an index. We compute now the price $c_{T,K}(t, S^{\delta_*}_t)$ of a fair European call option on the index with strike K and maturity T under the MMM. From the real world pricing formula (10.4.1) it follows that

$$\begin{aligned} c_{T,K}(t, S^{\delta_*}_t) &= S^{\delta_*}_t\, E\left(\frac{(S^{\delta_*}_T - K)^+}{S^{\delta_*}_T}\,\middle|\,\mathcal{A}_t\right) \\ &= E\left(\left(S^{\delta_*}_t - \frac{K\,S^{\delta_*}_t}{S^{\delta_*}_T}\right)^+\,\middle|\,\mathcal{A}_t\right) \end{aligned} \tag{13.3.16}$$

for $t \in [0,T]$. By applying the transition density of the time transformed squared Bessel process $\bar{S}^{\delta_*}$ of dimension four it has been shown in Hulley, Miller & Platen (2005) that the fair price of a European call option has the explicit formula

$$c_{T,K}(t, S^{\delta_*}_t) = S^{\delta_*}_t\,\left(1-\chi^2(d_1;4,\ell_2)\right) - K\,\exp\{-r\,(T-t)\}\,(1-\chi^2(d_1;0,\ell_2)) \tag{13.3.17}$$

with

$$d_1 = \frac{4\,\eta\,K\,\exp\{-r\,(T-t)\}}{S^0_t\,\alpha^{\delta_*}_t\,(\exp\{\eta\,(T-t)\}-1)} \tag{13.3.18}$$

and

$$\ell_2 = \frac{2\,\eta\,S_t^{\delta_*}}{S_t^0\,\alpha_t^{\delta_*}\,(\exp\{\eta\,(T-t)\}-1)} \tag{13.3.19}$$

for $t \in [0, T)$. This is an analytic pricing formula that involves the non-central chi-square distribution function, see (1.2.13). This formula has a similar level of complexity to that of the Black-Scholes formula, see (8.3.2). However, it provides more realistic European call option prices, as we shall see later.

We have shown in Fig. 12.3.1 an implied volatility surface for European call options on the GOP under the MMM. We noted a negatively skewed and slightly upwards sloping implied volatility surface.

European Put Options under the MMM

For completeness, let us now determine the fair price of a European put option on the GOP when the underlying model is the stylized MMM. For this purpose it is appropriate to use the fair put-call parity relation (12.2.60) to calculate the put price $p_{T,K}(t, \bar{S}_t^{\delta_*})$ at time t for maturity T and strike K. This means that we apply the formula

$$p_{T,K}(t, \bar{S}_t^{\delta_*}) = c_{T,K}(t, \bar{S}_t^{\delta_*}) - S_t^{\delta_*} + K\,P(t,T) \tag{13.3.20}$$

for $t \in [0, T)$. This leads us by (13.3.17) to the explicit European put formula

$$\begin{aligned} p_{T,K}(t, S_t^{\delta_*}) = &-S_t^{\delta_*}\left(\chi^2(d_1; 4, \ell_2)\right) \\ &+ K\,\exp\{-r\,(T-t)\}\left(\chi^2(d_1; 0, \ell_2) - \exp\{-\ell_2\}\right) \end{aligned} \tag{13.3.21}$$

for $t \in [0, T)$ when using the previous notation, see Hulley et al. (2005). One can calculate the implied volatilities for these put option prices as in Sect. 12.3. These are the same as those for the corresponding call prices.

As previously explained in Sect. 12.2, for the case of the modified CEV model, put-call parity breaks down if one uses the savings bond $P_T^*(t) = \frac{S_t^0}{S_T^0}$ instead of the fair bond $P(t,T)$ in relation (13.3.20).

It can be seen from (13.3.21) that when the GOP becomes very small, the put value also becomes small. As we have seen in (12.2.70), a put price derived under standard risk neutral pricing would be larger than the fair put price and would typically not become small when the GOP becomes small.

Note that one can explicitly calculate the forward price of a fair portfolio under the stylized MMM, as described at the end of Sect. 10.4. Furthermore, there are explicit formulas for fair European call and put options on primary security accounts, as will be discussed in Sect. 14.4.

13.4 MMM with Random Scaling (*)

Model Formulation (*)

The version of the MMM described here, which generalizes the stylized version derived in Sect. 13.2, is governed by a particular choice of the discounted GOP

drift $\alpha_t^{\delta_*}$. By (13.1.14) it can be seen that the $\alpha_t^{\delta_*}$, when integrated over time, yield the underlying value. One could argue that the underlying value is a non-decreasing, slowly varying stochastic process, where the randomness is caused by random trading activity potentially involving speculation.

If we take $\alpha_t^{\delta_*}$ to be a deterministic exponential function of time, as in (13.2.1), then we obtain the discounted GOP as a time transformed squared Bessel process of dimension $\delta = 4$. One could interpret this as an ideal or optimal market dynamics. Here $\alpha_t^{\delta_*}$ would express at time t the discounted underlying value that is transferred per unit of time into the market. The discounted GOP evolves due to the conservation of underlying value according to a very specific probability law. Interestingly, the underlying value plays here the role of a transforming time, see (13.3.3).

In order to capture some possible delays or accelerations of this transfer of discounted underlying value into the market, we now employ a squared Bessel process with a more general dimension $\delta > 2$ and allow also for some randomness in its time transformation.

This is achieved by introducing the process $Z = \{Z_t, t \in [0, \infty)\}$ via the power transformation

$$Z_t = \left(\bar{S}_t^{\delta_*}\right)^{\frac{2}{\delta-2}} \tag{13.4.1}$$

for $t \in [0, \infty)$ and $\delta \in (2, \infty)$. The Itô formula applied to (13.1.8) and (13.4.1) yields

$$dZ_t = \frac{\delta}{4}\,\gamma_t\,dt + \sqrt{\gamma_t\,Z_t}\,dW_t. \tag{13.4.2}$$

The *scaling process* $\gamma = \{\gamma_t, t \in [0, \infty)\}$ with

$$\gamma_t = Z_t\,\frac{\alpha_t^{\delta_*}}{\bar{S}_t^{\delta_*}}\,\frac{4}{(\delta-2)^2} \tag{13.4.3}$$

will be specified later in an appropriate manner to reflect realistically the randomness of market activity or market time observed in the market. This means that Z is a time transformed squared Bessel process of dimension $\delta > 2$, see Sect. 8.7. Note that for the standard choice $\delta = 4$ and $\gamma_t = 1$ we recover the stylized MMM, see Sect. 13.2. As we shall see, structuring the model equations in the above general form has the advantage that the model with deterministic γ_t can generate different slopes of the implied volatility surface for European call and put options via the dimension δ, see Heath & Platen (2005b).

Using the Itô formula together with (13.4.1) and (13.4.2), the GOP $S_t^{\delta_*}$ can be shown to satisfy the SDE

$$\begin{aligned} dS_t^{\delta_*} = S_t^{\delta_*} \Bigg(& \left[r + \left(\frac{\delta}{2} - 1\right)^2 \gamma_t \left(\frac{S_t^{\delta_*}}{S_t^0}\right)^{\frac{2}{2-\delta}} \right] dt \\ & + \left(\frac{\delta}{2} - 1\right) \sqrt{\gamma_t} \left(\frac{S_t^{\delta_*}}{S_t^0}\right)^{\frac{1}{2-\delta}} dW_t \Bigg) \end{aligned} \tag{13.4.4}$$

for $t \in [0, \infty)$. For simplicity, we assume a constant short rate $r_t = r \geq 0$. The GOP volatility or total market price of risk is by (13.1.1) and (13.4.1) of the form

$$|\theta_t| = \left(\frac{\delta}{2} - 1\right) \sqrt{\frac{\gamma_t}{Z_t}} \tag{13.4.5}$$

for $t \in [0, \infty)$. This means that the volatility of the GOP is stochastic and depends at time t on both the level of the discounted GOP with

$$\bar{S}_t^{\delta_*} = Z_t^{\frac{\delta-2}{2}} \tag{13.4.6}$$

and the random scaling quantity γ_t. Furthermore, the discounted GOP drift is by (13.1.4) and (13.4.5) given by

$$\alpha_t^{\delta_*} = \left(\frac{\delta}{2} - 1\right)^2 \gamma_t \, Z_t^{\frac{\delta-4}{2}} \tag{13.4.7}$$

for $t \in [0, \infty)$. By introducing a random scaling process, we model the discounted GOP drift in the form (13.4.7). Note that for the standard case with $\delta = 4$ the discounted GOP drift does not depend on Z_t. For $\delta > 4$ the discounted GOP drift increases when $\bar{S}_t^{\delta_*}$ increases. In the case $\delta \in (2, 4)$ the discounted GOP drift decreases when $\bar{S}_t^{\delta_*}$ increases.

Random Scaling (*)

The random scaling process can be used to model the typical short term features of the market. For instance, it can model various random and seasonal features of trading activity. We assume here that the scaling process $\gamma = \{\gamma_t, t \in [0, \infty)\}$ is a nonnegative, adapted stochastic process that satisfies an SDE of the form

$$d\gamma_t = a(t, \gamma_t)\, dt + b(t, \gamma_t) \left(\varrho \, dW_t + \sqrt{1 - \varrho^2}\, d\tilde{W}_t\right) \tag{13.4.8}$$

for $t \in [0, \infty)$ with a random initial value $\gamma_0 > 0$. Here $\tilde{W}$ is a Wiener process that models some uncertainty in trading activity and is assumed to be independent of W. The scaling drift $a(\cdot, \cdot)$ and scaling diffusion coefficient $b(\cdot, \cdot)$ are given functions of time t and scaling level γ_t. The scaling correlation ϱ is, for simplicity, assumed to be constant. Under this formulation the dynamics of the diffusion process γ can be chosen to match empirical evidence. Note that there seems to be no compelling reason to make the scaling correlation ϱ different to zero, see Breymann, Kelly & Platen (2006). The main feedback effect for indices, is well captured under the MMM already. We keep ϱ still flexible in the above model since it makes it similar to the stochastic volatility models presented in the previous section. For the preferred case $\varrho = 0$ we have independence between γ_t and W_t, which simplifies the computation of derivative prices.

The above MMM with random scaling offers different choices for the dimension $\delta > 2$ and, thus, different volatility dynamics. It has some similarity with the CEV model, see Sect. 12.2, which also involves a squared Bessel process. In Heath & Platen (2003) the random scaling was chosen to be a geometric Brownian motion, whereas in Heath & Platen (2005a) the dynamics are similar to those outlined above. The results for short term and medium term options are similar to those that we are going to report in this section.

We provide now an example for the modeling of random scaling that is motivated by an intraday empirical analysis of trading activity, obtained in Breymann et al. (2006) for a diversified world stock index denominated in US dollars. The scaling is modeled as a product of the type

$$\gamma_t = \xi_t \, m_t \tag{13.4.9}$$

with

$$\xi_t = \xi_0 \, \exp\{\eta \, t\} \tag{13.4.10}$$

for $t \in [0, \infty)$ with $\xi_0 > 0$. As before, the parameter $\eta > 0$ is called the net growth rate. The *market activity* process $m = \{m_t, t \in [0, \infty)\}$ in (13.4.9) is designed to model normalized trading activity. Note that for constant market activity $m_t = 1$ and dimension $\delta = 4$ the stylized MMM of Sect. 13.2 is recovered. In Breymann et al. (2006) it was suggested that market activity appears to have multiplicative noise. Therefore, the market activity process is modeled as a nonnegative process that satisfies an SDE of the form

$$dm_t = k(m_t) \, \beta^2 \, dt + \beta \, m_t \left(\varrho \, dW_t + \sqrt{1 - \varrho^2} \, d\tilde{W}_t \right) \tag{13.4.11}$$

for $t \in [0, \infty)$ with random initial market activity $m_0 \geq 0$. In this SDE multiplicative noise is characterized by the constant *activity volatility* $\beta > 0$. The function $k(\cdot)$ controls the drift of the market activity. Let us choose this function to be of the form

$$k(m) = (p - g \, m) \, \frac{m}{2}, \tag{13.4.12}$$

with speed of adjustment parameter g and reference level p. These constant, deterministic parameters are set so that the expected value of market activity is about one. The market activity process $m = \{m_t, t \in [0, \infty)\}$ has a stationary density, see (4.5.5), of the form

$$p_m(y) = \frac{g^{p-1}}{\Gamma(p-1)} \, y^{p-2} \exp\{-g \, y\} \tag{13.4.13}$$

for $y \in [0, \infty)$, where $\Gamma(\cdot)$ is the gamma function. This is a gamma density with mean $\frac{p-1}{g}$ and variance $\frac{1}{g}$ for parameters $p > 1$ and $g > 0$, see (1.2.9).

Figure 13.4.1 shows the stationary density (13.4.13) of m_t for different levels of market activity y and speed of adjustment parameter g, with $p = g+1$,

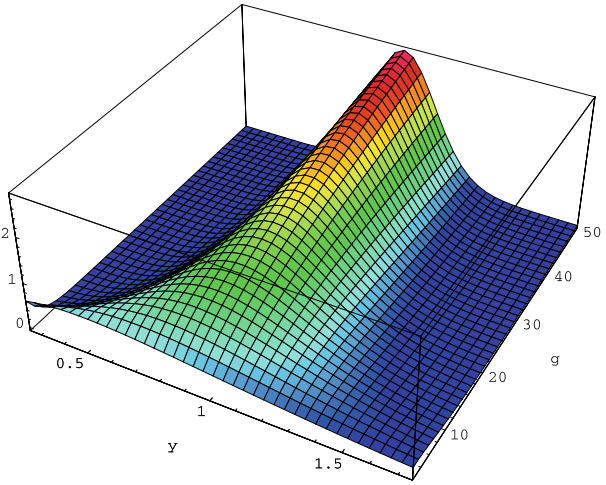

Fig. 13.4.1. Stationary density of market activity $m_t = y$ as function of y and speed of adjustment parameter g

to ensure that the mean of the stationary density always equals one. Note that for a large speed of adjustment parameter the market activity remains close to one.

Applying the Itô formula and using (13.4.9)–(13.4.12), the drift and diffusion coefficients appearing in (13.4.8) take the form

$$a(t,\gamma) = \gamma \left(p - g \frac{\gamma}{\xi_t} \right) + \gamma \eta \tag{13.4.14}$$

and

$$b(t,\gamma) = \beta \gamma, \tag{13.4.15}$$

respectively, for $t \in [0,\infty)$.

Note that at any time $t \in [0,\infty)$ the actual value of the market activity m_t, and thus the random scaling γ_t, are not easily observable. These change very rapidly and can only be estimated after sufficient time has elapsed. Therefore, the initial value m_0 of the market activity itself may have to be modeled as a random variable. For instance, the stationary density (13.4.13) could be used as its probability density. In the following we shall discuss the impact of using different parameter choices on various derivatives.

Zero Coupon Bond (*)

First, we consider a fair zero coupon bond that pays one unit of the domestic currency at the maturity date $T \in [0,\infty)$. An equivalent risk neutral probability measure does not exist for the above model. The benchmarked savings account $\hat{S}^0$ and, thus, the candidate Radon-Nikodym derivative process $\Lambda = \{\Lambda_t,\, t \in [0,\infty)\}$ with

$$\Lambda_t = \left(\frac{\bar{S}_t^{\delta_*}}{\bar{S}_0^{\delta_*}} \right)^{-1} = \left(\frac{Z_t}{Z_0} \right)^{1-\frac{\delta}{2}} \tag{13.4.16}$$

are by (8.7.24) strict local martingales when we assume no correlation, that is $\varrho = 0$. For this reason we shall use real world pricing to calculate derivative prices. By using (13.4.1) the benchmarked price $\hat{P}_T(t, Z_t, \gamma_t)$ for a zero coupon bond at time t with maturity T is then given by the conditional expectation

$$\hat{P}_T(t, Z_t, \gamma_t) = E\left(\frac{1}{S_T^{\delta_*}} \,\middle|\, \mathcal{A}_t \right) = E\left(\frac{1}{S_T^0 \, Z_T^{\frac{\delta}{2}-1}} \,\middle|\, \mathcal{A}_t \right) \tag{13.4.17}$$

for $t \in [0, T]$, see (10.4.8). Hence the corresponding zero coupon bond price $P_T(t, Z_t, \gamma_t)$ is given by

$$P_T(t, Z_t, \gamma_t) = S_t^{\delta_*} \, \hat{P}_T(t, Z_t, \gamma_t) = S_t^0 \, Z_t^{\frac{\delta}{2}-1} \, \hat{P}_T(t, Z_t, \gamma_t) \tag{13.4.18}$$

for $t \in [0, \infty)$.

In general, we do not have an explicit joint density of (Z_T, γ_T), which we would need to calculate the conditional expectation in (13.4.17). Therefore, let us introduce the diffusion operator $\mathcal{L}^0$ for the Markovian factors (Z_t, γ_t), which when applied to a sufficiently smooth function $f : (0, T) \times (0, \infty)^2 \to \Re$ is of the form

$$\begin{aligned} \mathcal{L}^0 f(t, Z, \gamma) = \Bigg(& \frac{\partial}{\partial t} + \frac{\delta \gamma}{4} \frac{\partial}{\partial Z} + a(t, \gamma) \frac{\partial}{\partial \gamma} + \frac{1}{2} \gamma Z \frac{\partial^2}{\partial Z^2} \\ & + \varrho \, b(t, \gamma) \, \gamma^{\frac{1}{2}} \, Z^{\frac{1}{2}} \frac{\partial^2}{\partial Z \, \partial \gamma} + \frac{1}{2} b(t, \gamma)^2 \gamma \frac{\partial^2}{\partial \gamma^2} \Bigg) f(t, Z, \gamma) \end{aligned} \tag{13.4.19}$$

for $(t, Z, \gamma) \in (0, T) \times (0, \infty)^2$. Using (13.4.2) and (13.4.8) together with the Feynman-Kac formula, see Sect. 9.7, the benchmarked fair zero coupon bond pricing function $\hat{P}_T(\cdot, \cdot, \cdot)$ satisfies the Kolmogorov backward equation

$$\mathcal{L}^0 \, \hat{P}_T(t, Z, \gamma) = 0 \tag{13.4.20}$$

for $(t, Z, \gamma) \in (0, T) \times (0, \infty)^2$ with terminal condition

$$\hat{P}_T(T, Z, \gamma) = \frac{1}{S_T^0 \, Z^{\frac{\delta}{2}-1}} \tag{13.4.21}$$

for $(Z, \gamma) \in (0, \infty)^2$. By using numerical methods for solving partial differential equations (PDEs), as we shall describe in Sect. 15.7, one can numerically determine $\hat{P}_T(\cdot, \cdot, \cdot)$.

Forward Rates (*)

For the above two-factor model we obtain by (10.4.12) the forward rate for the maturity date T at time $t < T$ by the formula

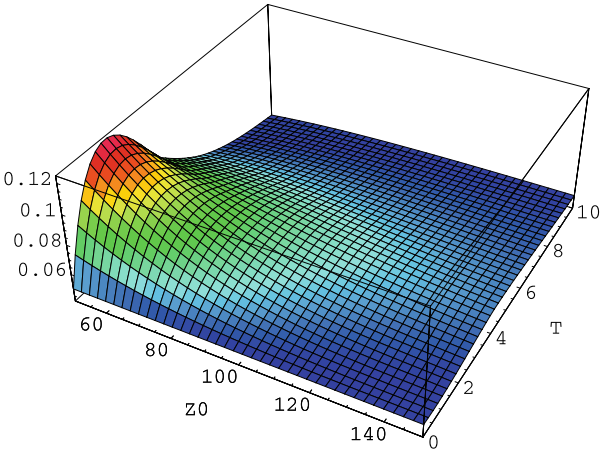

Fig. 13.4.2. Forward rates as a function of Z_0 and T

$$f_T(t, Z_t, \gamma_t) = -\frac{\partial}{\partial T} \ln\left(P_T(t, Z_t, \gamma_t)\right). \tag{13.4.22}$$

Figure 13.4.2 shows for different initial values of $Z_0 \in [50, 150]$ the forward rate curves at time $t = 0$ as functions of $T \in [0.25, 10]$. For this and subsequent plots the default parameters used are: $\delta = 4$, $r = 0.05$, $\varrho = 0$, $\eta_t = 0.048$, $\xi_0 = 10$, $p = 3$ and $g = 2$. Note that despite a constant short rate the forward rates are not constant and are always greater than the short rate. Furthermore, we observe a hump in the forward rate at about the time of two years to maturity. This is an important feature that has been observed in the market, see, for instance Bouchaud, Sagna, Cont, El Karoui & Potters (1999) and Matacz & Bouchaud (2000). These results together with those described below are numerically obtained by using the Crank-Nicolson finite difference method, which will be discussed in Sect. 15.7. The randomness of the initial value m_0 is generated by a two-point distributed random variable with mean $\frac{p-1}{g}$ and variance $\frac{1}{g}$. The fact that the realistic hump shaped forward rates, shown in Fig. 13.4.2, are greater than the constant short rate, demonstrates that the benchmarked savings account process $\hat{S}^0$, see (10.3.1), is a strict $(\underline{\mathcal{A}}, P)$-supermartingale, as was pointed out earlier.

European Options on a Market Index (*)

As previously explained, the GOP is employed as proxy for a market index. Consider now a European put option on the index S^{δ_*} with strike K and maturity date $T \in [0, \infty)$. Using the real world pricing formula (10.4.1), the put option price $p_{T,K}(t, Z_t, \gamma_t)$ is given by

$$p_{T,K}(t, Z_t, \gamma_t) = S_t^0 \, Z_t^{\frac{\delta}{2}-1} \, E\left(\left(\frac{K}{S_T^0 \, Z_T^{\frac{\delta}{2}-1}} - 1\right)^+ \Big| \mathcal{A}_t\right) \tag{13.4.23}$$

for $t \in [0, T]$.

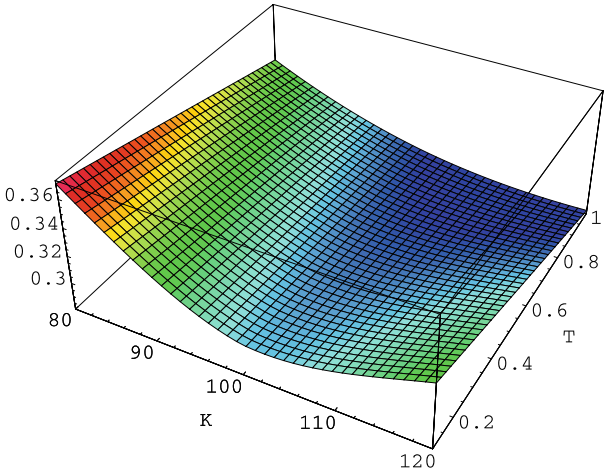

Fig. 13.4.3. Implied volatilities for put options on index as a function of strike K and maturity T

To see the effect of random scaling on implied volatilities, Fig. 13.4.3 displays an implied volatility surface for European puts as a function of the maturity date T and the strike K. These results were obtained using the zero coupon bond price (13.4.18) to infer the discount factor used in the Black-Scholes formula via (12.2.57). The implied volatilities shown in Fig. 13.4.3 are rather close to those observed for European index options in real markets, see Fig. 12.1.5. Note that the curvature of the implied volatility surface for short dated options results from the randomness of the scaling. One can show that this curvature is mainly generated by the randomness of the initial value m_0 of the market activity process. If a fixed initial value m_0 were used, then much of the curvature for the short dated implied volatility surface would disappear. This is important to notice since it tells us that the MMM with a random initial value already provides most of the stylized features observed in reality. The MMM with random initial scaling is also able to capture realistic implied volatility smiles for exchange rate and equity options, as observed in real markets, see Heath & Platen (2005a).

It is well-known that skew and smile patterns for implied volatility surfaces, as shown in Fig. 13.4.3, can be obtained by various stochastic volatility models, see Carr & Wu (2003) or Brigo, Mercurio & Rapisarda (2004) and our comments in Sect. 12.4. However, most of these models are difficult to calibrate to a range of standard and exotic derivatives. It has been demonstrated in Heath & Platen (2005a, 2005b) that the MMM avoids most of these problems.

To demonstrate the effect of making the scaling process γ stochastic, Fig. 13.4.4 shows implied volatilities for European puts on the GOP as a

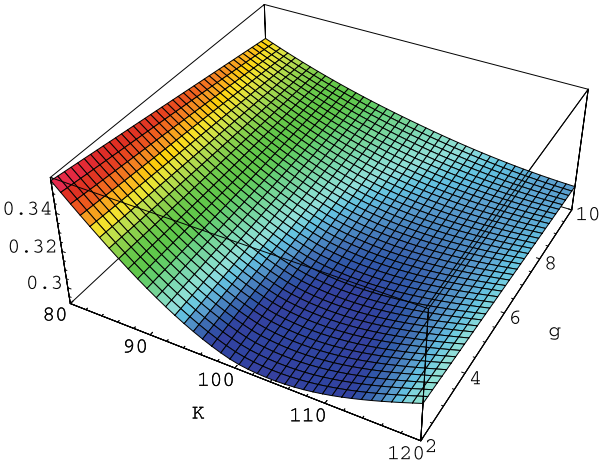

Fig. 13.4.4. Implied volatilities for put options as a function of strike K and speed of adjustment g

function of the strike K and the speed of adjustment parameter g for a fixed maturity date $T = 0.25$ and with $p = g + 1$. The figure indicates that an increase in speed of adjustment g decreases the curvature of the implied volatility curve, when viewed as a function of the strike K. For different values of g the corresponding initial random market activity m_0 is also adjusted to match the mean and variance of the corresponding stationary distribution.

It should be noted that changing the dimension δ of the time transformed squared Bessel process Z affects the slope of the implied volatility surface. That is, lowering the dimension δ produces a stronger negative skew for the implied volatility surface and vice versa.

For long dated European put or call options it can be seen that there is little curvature in the corresponding implied volatility curves for a given maturity date, see Fig. 13.4.5.

Note that a remarkably sustained increase in overall implied volatilities occurs for longer maturities. This is not usually obtained from a stochastic volatility model where an equivalent risk neutral probability measure exists. It can be observed that the impact of using random scaling, which is mainly reflected in the curvature of implied volatilities for short dated options, is not so prominent for longer dated maturities. This suggests that for long dated options deterministic scaling will suffice.

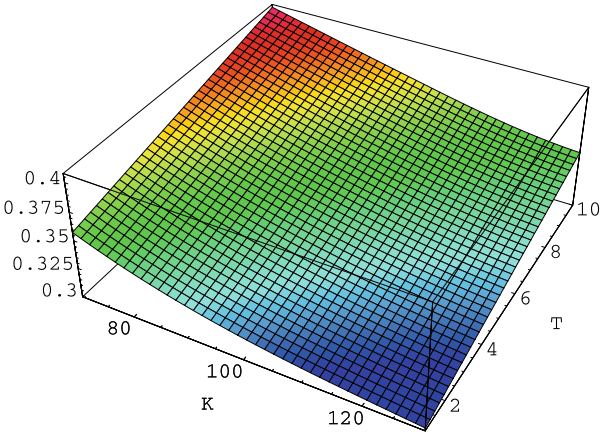

Fig. 13.4.5. Implied volatilities for long dated put options as a function of strike K and maturity T

13.5 Exercises for Chapter 13

13.1. Calculate the SDE for the logarithm of the discounted GOP.

13.2. Derive the SDE of the square root for the discounted GOP.

13.3. Derive the SDE for the normalized GOP $Y_t = \frac{\bar{S}_t^{\delta_*}}{\alpha_t^{\delta_*}}$ if

$$\alpha_t^{\delta_*} = \alpha_0 \, \exp\{\int_0^t \eta_s \, ds\}.$$

13.4. Calculate the SDE for the squared volatility of the discounted GOP, given as in Exercise 13.3.